論文内容の要旨

Metal–Macrocycle Frameworks: Porous Supramolecular Crystals with Multiple Molecular Receptors on the Pore Surfaces

（金属マクロサイクル集積体：
細孔表面に多種の分子レセプターを有する多孔性超分子結晶の創製）

窪田　亮

1. Introduction

Molecular-sized spaces formed within self-assembled hollow nano-structures, such as capsules, micelles/vesicles, and porous crystals, have attracted considerable attention due to their specific spatial functions for molecular encapsulation, separation, transportation, and transformation. In order to enhance selectivity and efficiency of these spatial functions, it is of significant importance to precisely control the size, shape, and chemical and physical properties of the interior surfaces of the nano-space. In line with this concept, a novel strategy is required for the arrangement of multiple functional groups in an accurately-oriented way at desired positions of the interior surface. However, it has long been a challenge to arrange a variety of molecular recognition sites on the surface in a site-selective manner. To realize this, I envisioned that self-assembly of metallo-macrocyclic compounds would provide novel porous crystalline materials with well-defined molecular receptors arising from the macrocyclic cavities on the inner pore surfaces.

In this study, I have synthesized a family of porous crystalline materials, Metal–Macrocycle Frameworks (MMFs), composed of one, two, or four stereoisomers of trinuclear macrocyclic Pd^{II} complexes. These MMFs possess nano-sized pores surrounded by a variety of molecular binding pockets on the interior surfaces. The chemical and physical properties of the MMF surface can be adjusted by site-selective, reversible surface modification simply by soaking in a solvent containing organic/inorganic guest molecules. Notably, not only the size and shape of the pore but also the binding modes of guest molecules can be tuned by solvent-induced pseudopolymorphism of the MMFs. Furthermore, asymmetric crystallization of the MMFs was induced by optically-active sugar-derived lactones, generating chirality of the pore and the binding pockets of the MMFs.

2. Synthesis of Metal–Macrocycle Framework 1

A porous Metal–Macrocycle Framework **1** (**MMF-1**) with five kinds of enantiomeric-paired binding pockets was constructed from a structurally flexible tris-bidentate macrocyclic ligand **L** and $PdCl_2(CH_3CN)_2$. Complexation of ligand **L** and 3 equiv. of $PdCl_2(CH_3CN)_2$ in CH_3CN produces yellow single-crystals in 41% yield which consist of an equal amount of four stereoisomers of neutral trinuclear macrocyclic Pd^{II} complexes, $Pd_3\mathbf{L}Cl_6$ (Figure 1a). In the two conformational isomers (*Syn* and *Anti*), all the three or two Pd^{II} centers, respectively, are located on the same side of the macrocyclic ligand (Figures 1b,c). For each isomer, two helical structures (*P* and *M*) are induced by intramolecular, circularly-oriented three C-H---π interactions (Figure 1d). Moreover, each trinuclear Pd^{II} macrocyclic complex has a pair of guest binding pockets on their top and bottom faces, head- and tail-Pockets, respectively. In the crystal formed in CH_3CN, the four isomers are regularly arranged mainly through N-H---Cl hydrogen bonding and Pd-Pd interactions to construct a rectangular nano-channel structure with the size of 1.4×1.9 nm^2 (Figure 1e). This nano-channel can provide five enantiomerically-paired guest binding pockets on the pore surface.

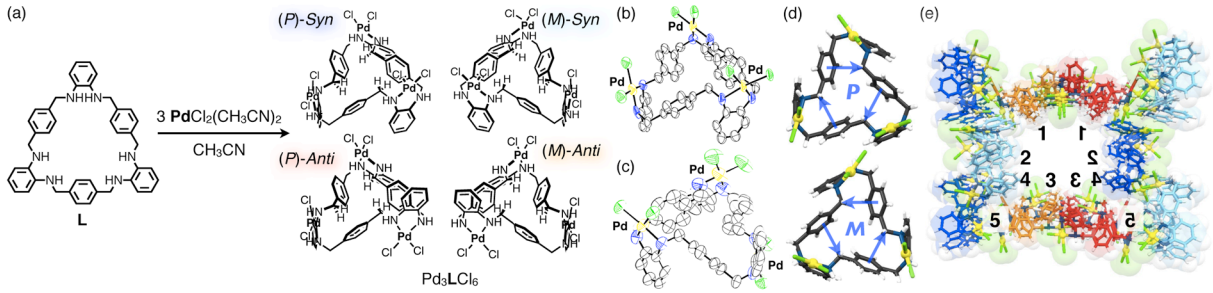

Figure 1. (a) Complexation of ligand **L** and 3 equiv. of $PdCl_2(CH_3CN)_2$. ORTEP drawings of (b) (*P*)-*Syn* and (c) (*M*)-*Anti* isomers at 50% probability level. (d) Helical structures of (*P*/*M*)-*Syn* isomers. Pd, yellow; Cl, green; N, blue; C, black. (e) A unit pore structure of **MMF-1** possessing five different enantiomerically-paired binding pockets. **1**: (*P*/*M*)-*Anti*-head Pockets, **2**: (*P*/*M*)-*Syn*-tail Pockets, **3**: (*P*/*M*)-*Anti*-tail Pockets, **4**: (*P*/*M*)-Ellipsoidal Pockets, **5**: (*P*/*M*)-Tubular Pockets. Carbon atoms for (*P*)-*Syn,* (*M*)-*Syn*, (*P*)-*Anti*, and (*M*)-*Anti* are shown in blue, aqua, red, and orange, respectively.

3. Site-selective guest adsorption to the MMF-1 surface

Adsorption behaviors of small aromatic molecules to the **MMF-1** surface were examined for the site-selective surface modification in a noncovalent manner. X-ray diffraction of a single-crystal, which was obtained as the result of the crystal-to-crystal transformation by the soaking of a single crystalline **MMF-1** in a 1:1 (v/v) mixed solvent of CH_3CN and benzene at 30 °C for one day, revealed that benzene molecules are included within two sets of binding pockets, (*P*/*M*)-*Anti*-head and (*P*/*M*)-*Syn*-tail Pockets, mainly through C-H---π interactions and van der Waals interactions (82% and 66% occupancies, respectively) (Figure 2a). Residual benzene molecules in the free pore space are highly disordered. Furthermore, other simple aromatic hydrocarbons, such as naphthalene and azulene, show different binding modes from that of benzene, indicating that the adsorption behaviors on the surface depend on the size and/or shape of guest molecules (Figure 2b).

To further assess the shape- and orientation-selectivities in the guest adsorption, three dibromobenzene isomers were selected as guests. Single-crystal X-ray analyses revealed that adsorption of dibromobenzene isomers is highly shape-selective on the **MMF-1** surface (Figures 2c-e). *O*-isomer is captured in the (*P*/*M*)-*Syn*-tail and (*P*/*M*)-Ellipsoidal Pockets (51% and 53%, respectively). On the other hand, *m*-isomer is trapped in the (*P*/*M*)-*Syn*-tail and (*P*/*M*)-*Anti*-head Pockets (52% and 89%, respectively), and *p*-isomer is included only in the (*P*/*M*)-Ellipsoidal Pockets (68%). It should be noted that every dibromobenzene isomer is oriented without fluctuation as confirmed by electron densities of heavy Br atoms. Subsequently, a solution containing a mixture of *m*- and *p*-dibromobenzenes in CH_3CN was used for binary guest arrangement. The crystal structure of **MMF-1** including *m*- and *p*-isomers shows that two guests are sorted in different binding pockets (Figure 2f). The binding selectivity of the dibromobenzene mixture is completely consistent with those of both individual isomers.

Furthermore, highly diastereoselective guest adsorption was achieved when using optically-active, disubstituted aromatic molecules, (1*R*)- or (1*S*)-1-(3-chlorophenyl)ethanol (Figures 2g,h). Single-crystal X-ray diffraction of a single crystal, which was obtained by the soaking of the **MMF-1** in a 1:2 (v/v) mixture of CH_3CN and (1*R*)-isomer at 30 °C for one day, revealed that the guest molecules are encapsulated in one of the enantiomerically-paired binding pockets. As is obvious, the (1*S*)-isomer is encapsulated into each mirror-image binding pocket. In the electron density map, there is no electron density assignable to the guest molecule in the other enantiomerically-paired binding pockets. This strongly suggests that the resulting diastereoselectivity is substantially high.

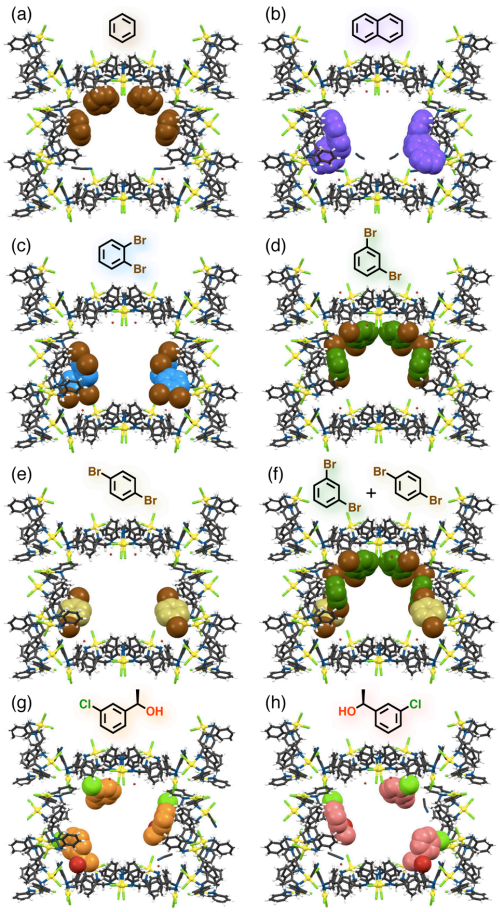

Figure 2. Unit pore structures of **MMF-1** including (a) benzene, (b) naphthalene, (c) *o*-, (d) *m*-, (e) *p*-dibromobenzene, (f) a mixture of *m*- and *p*-dibromobenzenes, (g) (1*R*)-, and (h) (1*S*)-1-(3-chlorophenyl)ethanol. Stick model: **MMF-1**, space-filling model: guest molecules.

4. Direct X-ray observation of a guest exchange process on the MMF-1 surface

In order to study adsorption kinetics of guest molecules on the **MMF-1** surface, the time-course X-ray analysis was conducted. Four successive single-crystal X-ray measurements allowed to visualize a guest exchange process at the molecular binding pockets. To make the guest exchange more slowly, the experiment was carried out at –180 °C, and the incubation for the guest exchange was conducted at –40 °C (Figures 3a,b). The crystal structures of the **MMF-1** crystal briefly-immersed into a 1:2 (v/v) mixed solvent of CH_3CN and (1*R*)-1-(3-chlorophenyl)ethanol at 23 °C for 5 min are shown in Figures 3c-f. Comparative study of the four structures indicated a slow guest exchange process in the (*P*)-*Syn*-tail Pocket. Moreover, an intermediate guest adsorption was clearly detected as indicated by arrows. These atomic level observations would provide a new insight into the kinetics of guest adsorption behaviors on the inner crystal surface.

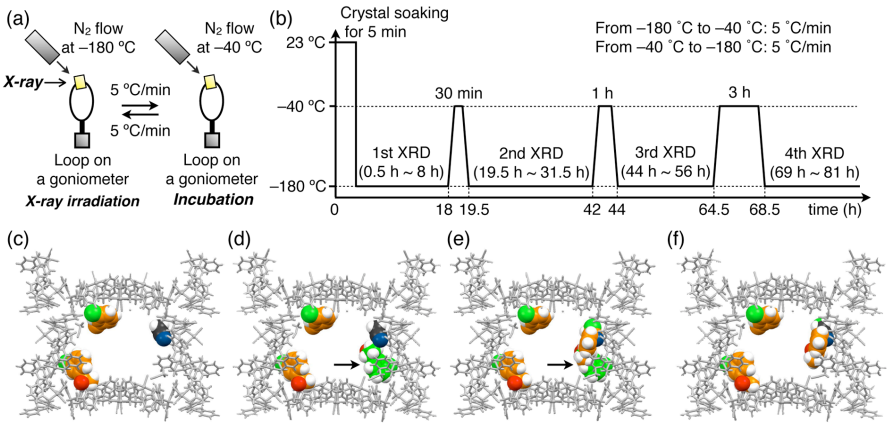

Figure 3. (a) Schematic illustration of the time-course X-ray diffraction of (1*R*)-1-(3-chlorophenyl)ethanol on a goniometer of the X-ray apparatus. (b) Detailed time table. XRD: single-crystal X-ray diffraction. Unit pore structures of the (c) 1st, (d) 2nd, (e) 3rd, and (f) 4th measurements. The carbon atoms of the intermediate guest molecule is shown in green and indicated by arrows.

5. Three-dimensionally interconnected pores: MMF-2

The trinuclear macrocyclic Pd^{II} complex, Pd_3**L**Cl_6, exhibits solvent-induced pseudopolymorphisms. One of them is **MMF-2**, which has a different size and shape of pore with different guest binding pockets on the surface from **MMF-1**. Complexation of ligand **L** and 3 equiv. of $PdCl_2(CH_3CN)_2$ in a 1:9 (v/v) mixed solvent of DMSO and CH_2Cl_2 generates yellow-orange single crystals of ***rac*-MMF-2** composed of only (*P*/*M*)-*Syn* isomers (Figure 4a). The single-crystal X-ray diffraction revealed that ***rac*-MMF-2** crystallizes in a chiral cubic space group, $I2_13$, with a Flack parameter 0.48(5), indicating that ***rac*-MMF-2** exists as a racemic mixed crystal. Namely, a unit cell of the ***rac*-MMF-2** crystal consists of one kind of stereoisomers of Pd_3**L**Cl_6, either a (*P*)- or an (*M*)-*Syn* isomer, but the ***rac*-MMF-2** as a whole contains an equal amount of both (*P*)- and (*M*)-*Syn* isomers. In ***rac*-MMF-2**, (*P*/*M*)-*Syn* isomers interact with each other through N-H---Cl hydrogen bonds (average N-Cl distance, 3.3 Å) and Pd-Pd interactions (Pd-Pd distance, 3.17 Å) to form three-dimensionally connected pores. In addition, ***rac*-MMF-2** has cylindrical nano-spaces with a diameter of 10 Å and a length of 7 Å surrounded by two types of the molecular binding pockets, *Syn*-head and -tail Pockets (Figure 4b).

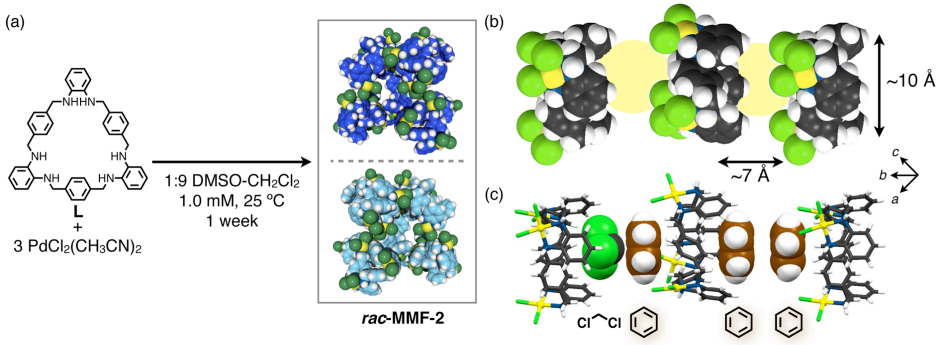

Figure 4. (a) Synthesis of ***rac*-MMF-2**. (b) Nano-sized space within ***rac*-MMF-2** surrounded by *Syn*-head and -tail Pockets. (c) Nano-sized space of ***rac*-MMF-2** containing benzene molecules. C, black; N, blue; Pd, yellow; Cl, green; H, white. Carbon atoms of the trapped benzene are shown in brown.

Moreover, ***rac*-MMF-2** can capture small organic molecules such as benzene and cyclohexane. Single-crystal X-ray analysis of a crystal, which was obtained after the soaking of crystalline **MMF-2** in a 1:1 (v/v) mixed solvent of benzene and CH_2Cl_2 revealed that benzene molecules are adsorbed to both *Syn*-head and -tail Pockets mainly through C-H---Cl hydrogen bonding and C-H---π interactions (Figure 4c). For uptake experiments with cyclohexane, only a *Syn*-head Pocket captures cyclohexane but with low occupancy of 17%. So in competition experiments, a selective uptake behavior of benzene over cyclohexane was observed for the ***rac*-MMF-2**. The crystals of ***rac*-MMF-2** were soaked into a CH_2Cl_2 solution of benzene and cyclohexane (1.0 M each) for one day at 30 °C, and then digested in

DMSO-d_6/DCl-D_2O. The ^{1}H NMR spectrum of the resulting mixture indicated that molar ratio of benzene and cyclohexane trapped in the **MMF-2** pores is 90:10, namely the selectivity of benzene uptake over cyclohexane is 9. Thus, the crystal structures and ^{1}H NMR spectroscopy suggest that **MMF-2** exhibits a high capability of molecular separation through the nano-space surrounded by the molecular binding pockets.

6. Asymmetric crystallization of MMF-2 with optically-active lactones

Asymmetric crystallization of **MMF-2** was achieved by chirality induction using optically-active sugar-derived lactones (Figure 5). Crystallization of Pd_3LCl_6 in a 1:9 (v/v) mixed solvent of DMSO and CH_2Cl_2 in the presence of 30 equiv. of D-glucono-1,5-lactone or 70 equiv. of D-glucurono-6,3-lactone produced homochiral **MMF-2** crystals, ***P*-MMF-2** or ***M*-MMF-2**, respectively. The single-crystal structures of ***P***- and ***M*-MMF-2** show that their unit cell structures are completely the same as that of ***rac*-MMF-2** and no chiral lactones as the asymmetric induction reagents were therefore included in the crystals. Importantly, the Flack parameters of ***P***- and ***M*-MMF-2** are 0.07(9) and 0.06(7), respectively, indicating high asymmetric induction. Thus, the optically-active lactones have influence not on the crystal structures, but on the asymmetric induction of the **MMF-2** crystals. The resulting chiral spaces could be applied for catalytic asymmetric reactions.

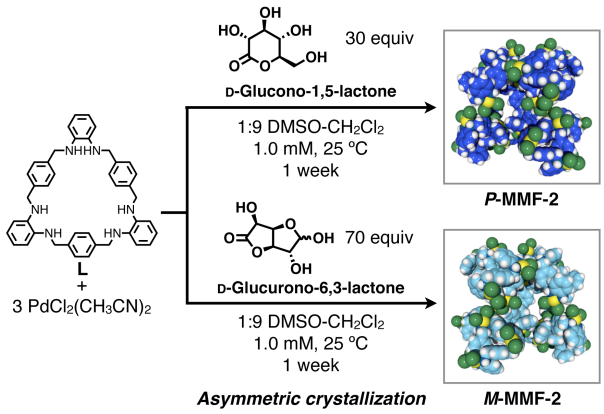

Figure 5. Asymmetric crystallization of **MMF-2** using optically-active sugar-derived lactones, D-glucono-1,5-lactone and D-glucurono-6,3-lactone.

7. Other pseudopolymorphisms of MMF; MMF-3 and MMF-4

The trinuclear Pd^{II} complexes show further solvent-induced pseudopolymorphisms to form two other types, **MMF-3** and **MMF-4** from a 1:9 (v/v) mixed solvent of DMSO and $CHCl_3$ (Figure 6a). These two different porous MMF crystals composed of (*P*/*M*)-*Syn* isomers are simultaneously formed as concomitant polymorphs from a 1:9 (v/v) mixed DMSO-$CHCl_3$ solution containing ligand **L** and 3 equiv. of $PdCl_2(CH_3CN)_2$. The crystal habit and packing structure of **MMF-3** are similar to those of ***rac*-MMF-2**. However, **MMF-3** crystallizes in an achiral cubic space group, $I\bar{4}3d$, and contains both (*P*)- and (*M*)-*Syn* isomers in a unit cell. For **MMF-4** whose unit cell also consists of both (*P*)- and (*M*)-*Syn* isomers, the packing structure is completely different from those of ***rac*-MMF-2** and **MMF-3** (Figure 6b). In **MMF-4**, (*P*)- and (*M*)-*Syn* isomers alternately are aligned in a head-to-tail manner along the *c* axis (Figure 6c). Furthermore, these columns of the (*P*/*M*)-*Syn* isomers make a hexagonal array in the packing structure to form a one-dimensional hexagonal nano-channel structure with a diameter of 1.2 nm.

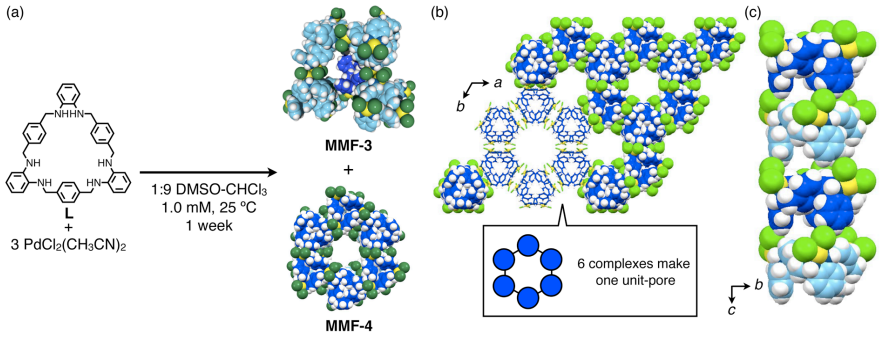

Figure 6. (a) Synthesis of **MMF-3** and **MMF-4** as concomitant polymorphs. (b) A hexagonal packing structure of **MMF-4**. (c) Head-to-tail columnar packing along the *c* axis of **MMF-4**. Carbon atoms of (*P*)-*Syn* and (*M*)-*Syn* isomers are represented by blue and aqua, respectively.

8. Conclusion

To develop functional supramolecular spaces, I have constructed a family of Metal–Macrocycle Frameworks from trinuclear macrocylic Pd^{II} complexes as the building blocks. The resulting self-assembled crystalline compounds have a variety of molecular binding pockets on their inner pore surfaces. Using these binding pockets, site-selective, reversible surface modification has been achieved with small aromatic organic molecules. Furthermore, the size and shape of the MMF pores and the types and chirality of the binding pockets on the surfaces can be controlled by solvent-induced pseudopolymorphisms and asymmetric crystallization in the presence of optically-active lactones. Such supramolecular, multi-functional spaces formed in MMF would show space-specific functions, such as molecular separation, highly efficient asymmetric catalytic reactions, and polymer formation.